Available online at www.sciencedirect.com

jmr&t Journal of Materials Research and Technology

journal homepage: www.elsevier.com/locate/jmrt

Original Article

Rheological properties of cement pastes with cellulose microfibers

Seongwoo Gwon [a,b], Myoungsu Shin [b,*]

[a] School of Civil and Environmental Engineering, Georgia Institute of Technology, Atlanta, GA, 30332, United States
[b] School of Urban and Environmental Engineering, Ulsan National Institute of Science and Technology (UNIST), 50 UNIST-gil, Ulsan, 44919, South Korea

ARTICLE INFO

Article history:
Received 11 November 2020
Accepted 20 December 2020
Available online 24 December 2020

Keywords:
Rheology
Natural fiber composites
Cellulose microfiber
Herschel–Bulkley fluid
Structural breakdown
Mini-slump flow

ABSTRACT

The rheological properties of cement pastes prepared using kenaf-plant cellulose microfibers (CMFs), which was incorporated for the purpose of internal curing, were investigated. The main test variables are the length and mass fraction of the CMFs. CMFs of lengths of 400 μm and 5 mm were included in the mixtures at 0.3, 0.6, 1, and 2 wt.% of the cement. Dry CMF particles were wetted with water to the fiber saturation point using vacuum filtration immediately before mixing. An optimum shearing protocol was designed to minimize the shear-induced structural breakdown of cement pastes with the CMFs under hysteresis loops of the shear strain rate. It consisted of an initial pre-shearing step at a high shear strain rate of 80 1/s, three acceleration and deceleration cycles with a maximum shear strain rate of 40 1/s, and a rest step before each acceleration. The mixtures' flow curves were well fitted to the Herschel–Bulkley fluid model with a minimum coefficient of determination of 0.9993. The yield stress of cement pastes was at least 34.3% higher for longer CMFs at the same dose. However, the mixtures exhibited similar plastic viscosities with a coefficient of variation of only approximately 5.8%.

1. Introduction

Plant-based cellulose fibers such as kenaf, jute, coconut, and hemp are commonly produced by the global agroindustry. Such fibers are abundantly cultivated from renewable sources and are cheaper than man-made synthetic fibers. Recently, approximately 68% of the global cellulose fibers market has been occupied by Asia–Pacific countries [1]. The global market size for cellulose fibers is projected to rapidly expand and reach 41.5 billion USD by 2025 [1]. Most of all, cellulose fibers are renewable resources that reduce the environmental impact of related products [2,3]. In particular, kenaf fibers are commercially available in the United States and Asia because they can be cultivated every 3–4 months at approximately 1.7 kg/m^2 [4]. Cellulose fibers are usually employed as feedstocks in many industries, ranging from the biomedical field to the polymer science field, as alternatives to some steel and

Abbreviations: CMF, cellulose microfibers; RH, relative humidity; SAPs, superabsorbent polymers; TG, thermogravimetry; DTG, derivative thermogravimetry; CMC, construction material cell.

* *Corresponding author.*
E-mail address: msshin@unist.ac.kr (M. Shin).

https://doi.org/10.1016/j.jmrt.2020.12.067

polymeric fibers [5–11]. They have also been used as additives in cement and concrete composites [12]. In particular, the use of cellulose fibers is known to modulate the cement setting time [13], autogenous shrinkage, and internal relative humidity (RH) [14,15], as well as the rheological properties of concrete [16], owing to their hygroscopicity and chemical composition.

Several researchers have investigated the mechanical and durability characteristics of cellulose fiber-reinforced cement composites with short or pulp fibers [17–19]. These characteristics are dependent on the source plants, fiber dose, fiber length, fiber processing, and the chemical condition of the fiber surface [20,21]. Incidentally, raw cellulose fibers exhibit a favorable performance in the internal curing of concrete with a reduced degree of self-desiccation and autogenous shrinkage [12,14,22], as was confirmed by superabsorbent polymers (SAPs) [23] and pre-wetted fine lightweight aggregate [24]. The majority of previous studies on internal curing comprised the use of short cellulose fibers [25–27]. It has been observed that changes in the rheological behavior as well as delays in the cement setting were due to the presence of the cellulose fibers. Similarly, the authors also found that both the change in the rheological properties and the cement setting delay manifested on using cellulose microfibers (CMFs), which were used for the purpose of internal curing [28]. However, the rheological properties of cement composites comprising cellulose fibers were barely quantitatively evaluated. Only Nilsson and Sargenius [29] investigated the rheological modification of cement mortars containing CMFs from recycled paper and superplasticizer. Moreover, cellulose fibers are different from synthetic fibers, in that the fiber size, water absorption capacity, and chemical dissolution can affect the hydration of the cement from an early age [13,30]. The use of CMFs for internal curing may significantly reduce the flowability of cement composites. However, studies on the effect of CMFs on the rheology of cement composites have not been reported thus far. Thus, a guideline is required for evaluating the rheological properties of cement composites comprising cellulose fibers.

Considering the requirement for the evaluation of the rheology of cement composites comprising cellulose fibers, in this study, the rheological properties of cement pastes comprising CMFs of two lengths were investigated. The mix proportions of all the cement pastes were selected from a previous study on the internal curing of cement composites using CMFs [28]. The main test variables were the length and mass fraction of the CMFs. All the CMF particles were wetted with water up to the fiber saturation point using vacuum filtration before mixing. Thus, except for the CMFs in the plastic state, it was assumed that the CMFs did not alter the water/cement (w/c) ratio of cement pastes. Before the design of the shearing protocol, it was observed that the shear-stress level of all the mixtures decreased under repeated normal shearing cycles that comprised only the acceleration and deceleration of the shear strain rate. This phenomenon was associated with a shear-induced structural breakdown, i.e., the structure does not recover owing to the breakage of the membranes or chemical linkages between the cement particles [31]— which are assumed to be formed during the cement hydration—due to shear. Thus, an optimal shearing protocol was designed to minimize the occurrence of a structural breakdown.

The main purpose of this study is to present a reference guideline for evaluating the rheological properties of cement pastes comprising CMFs. This study comprehensively conducted the preparation and processing of CMFs and the optimal design of shearing protocol, as well as the evaluation of the rheological properties of cement pastes with CMFs. Two types of CMFs with lengths of 400 μm and 5 mm were incorporated into the cement pastes at 0.3, 0.6, 1, and 2 wt.% of cement. Following the designed shearing protocol consisting of an initial pre-shearing step at a high shear strain rate, three acceleration and deceleration cycles, and a rest step before each acceleration, the flow curves of all the mixtures were fitted to the constitutive equation of the Herschel–Bulkley (H–B) fluid model to evaluate their rheological properties [32]. Finally, based on the analysis, the shearing protocol designed in this study was found to be suitable for evaluating the rheological properties of cement pastes containing CMFs.

2. Test specimens

The mix proportions in this study were originally designed for investigating the effectiveness of plant CMFs as an internal curing agent in cement composites [28]. The main test variables are the length and mass fraction of the CMFs. The flow chart of this study is presented in Fig. 1.

2.1. *Materials*

In this study, cement, water, superplasticizer, and plant CMFs of two lengths were used to produce various mixtures of cement pastes. Type-I ordinary Portland cement with a

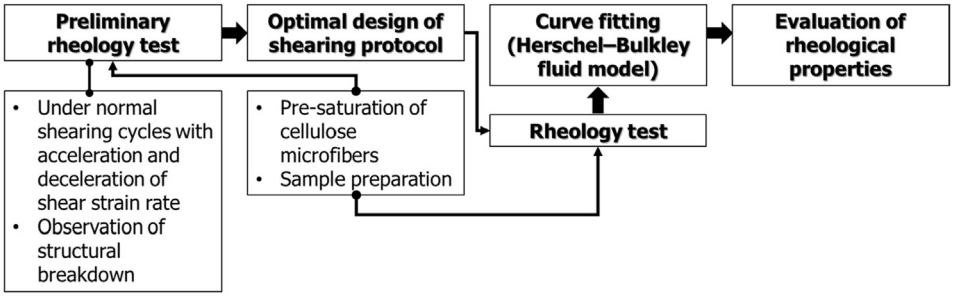

Fig. 1 – Flow chart of rheology study.

density of 3.13 g/cm^3 was used, and its particle size distribution, as measured using laser diffraction, is presented in Fig. 2. The chemical oxide composition of the cement, as determined using an X-ray fluorescence spectrometer (Bruker S8 Tiger, USA), is listed in Table 1. The loss on ignition of the cement was 2.31%. A polycarboxylate-based superplasticizer (specific gravity: 1.04±0.05, pH: 5.0±2.0) was used owing to its effectiveness in the dispersion of plant cellulose fibers in cement composites [14].

The two types of CMFs presented in Fig. 3 were manufactured by pulverizing original kenaf strand fibers with an average tensile strength of 330 MPa and oven-dried density of 1.36 g/cm^3 determined by direct tension test and automatic gas pycnometer, respectively. Pulverizers operating at 25,000 and 28,000 rpm were used to process the strand fibers into the CMFs, which were referred to as 1MF and 2MF, respectively (Fig. 3), where "MF" denotes microfibers. 1MF and 2MF had average lengths of 5 mm and 400 μm and porosities of 82.9% and 85.9%, respectively.

2.2. Chemical composition and thermogravimetric analysis

The chemical composition of the CMFs, determined via three repetitions of a method comprising fat removal and a series of filtrations [33], is listed in Table 2, which suggests that cellulose is the major component. The lignin showed the maximum standard deviation of 0.32 wt.% in the chemical composition. This was also confirmed by the thermogravimetric analysis of the kenaf powder (Fig. 4); a substantial decomposition of cellulose occurs at 300–400 °C (Fig. 4) [34].

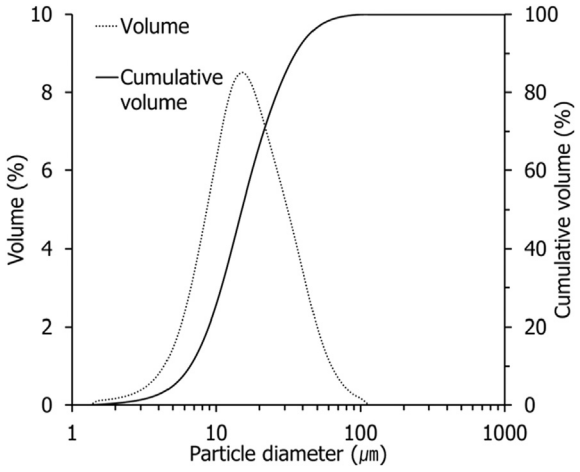

Fig. 2 – Particle size distribution of Portland cement.

Table 1 – Chemical oxide composition of Portland cement.

Oxide	Portland cement (wt.%)
CaO	61.72
SiO_2	21.32
Al_2O_3	5.61
Fe_2O_3	3.12
SO_3	2.51
MgO	3.94
K_2O	0.79
TiO_2	–
MnO	–

2.3. Mix proportions

Eight mix proportions of cement pastes, as presented in Table 3, were tested in this study. The amounts of dry CMFs varied from 0.3% to 2.0% of the cement by weight. In all the mixtures, the w/c ratio was 0.3, and the amount of superplasticizer was fixed at 1.3% of the cement by weight. The amount of superplasticizer was selected to ensure sufficient dispersion of the CMFs despite their different lengths and quantities. The maximum dose of dry CMFs was 2 wt.% of the cement, but the 2 wt.% 1MF case was excluded from the mix proportions owing to the accompanying agglomeration of fibers. For the preparation of the CMFs prior to the mixing, the dry CMF particles were wetted using water up to the fiber saturation point.

2.4. Pre-saturation of CMFs

To prepare the CMFs and wet them up to the fiber saturation point before mixing, a vacuum filtration setup with a Teflon (also called "polytetrafluoroethylene") membrane filter was employed (Fig. 5). The membrane filter had a diameter and sieve size of 47 mm and 0.45 μm, respectively. First, the dry CMF particles were placed in the funnel clamped onto the flask, and a membrane filter was fixed between the funnel and the flask. Water approximately ten times the weight of the dry CMFs was then poured into the funnel. Before operating the vacuum pump, the CMF particles were allowed to soak completely for approximately 10 min after the addition of water. Finally, a vacuum pump with a pressure of 490 mmHg was operated for approximately 5 min. The saturated CMF particles thus obtained were then ready for the mixing.

2.5. Sample preparation

Mixing was performed in a controlled room at 23 ± 2 °C and 50 ± 4% RH. First, the cement was dry mixed for approximately 30 s in a Hobart mixer set at 100 rpm. Meanwhile, the presaturated CMFs and a blend of water and superplasticizer were prepared for the mixing. The saturated CMFs were not included in the dry mixing because some portion of the water absorbed by the CMFs could be absorbed by the cement particles. After pouring the premixed blend of water and superplasticizer into the mixing bowl, wet mixing was continued for 60 s at 100 rpm. Finally, the saturated CMFs were added into the bowl, and the final mixing was performed for 6 min at 200 rpm to ensure uniform dispersion of the CMFs. The plastic mixture thus obtained was then used for the rheometer and mini-slump-flow tests.

3. Test methods

3.1. Rheometer test

A commercial rheometer (HAAKE MARS III, Thermo Fisher Scientific, USA) with a construction material cell (CMC) was

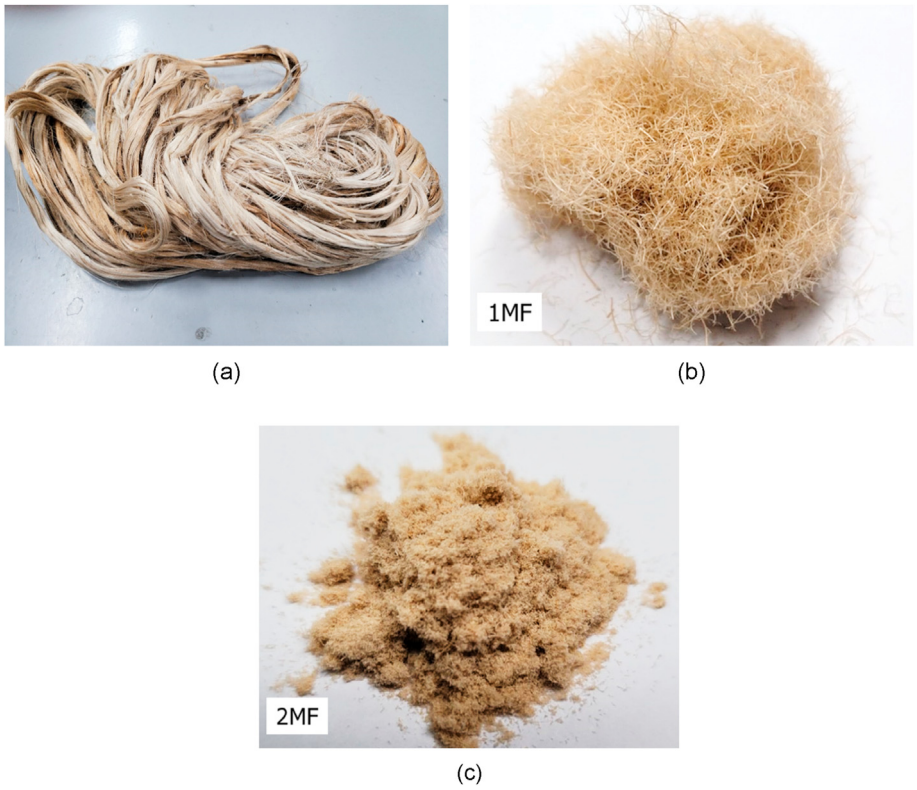

Fig. 3 – (a) Kenaf strand fibers and CMFs: (b) 1MF (approximate length of 5 mm), (c) 2MF (approximate length of 400 μm).

Table 2 – Chemical composition of kenaf CMFs (unit: wt.%).

Cellulose	Hemicellulose	Lignin	Extractives	Ash
54.1	29.3	14.3	0.8	1.4

used to evaluate the rheological properties of the cement pastes comprising CMFs (Fig. 6(a)). The CMC consisted of a two-bladed vane-and-cylinder container, which is presented in Fig. 6(b). Other types of rheometer cells, such as those comprising a concentric cylinder or parallel plates, were not

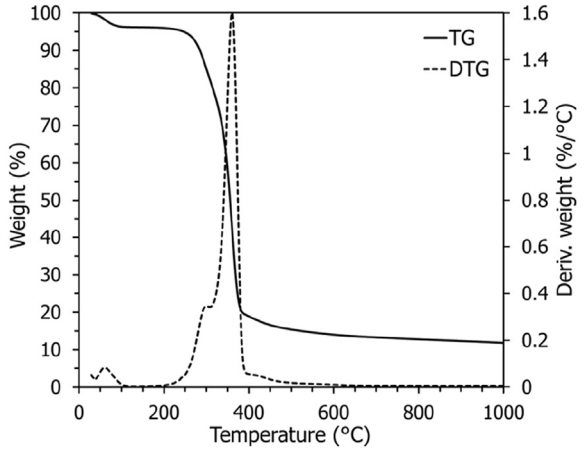

Fig. 4 – Thermogravimetry (TG) and derivative thermogravimetry (DTG) of kenaf CMF powder.

Table 3 – Mix proportions of tested cement pastes.

Mixture	Cement (kg/m^3)	Water (kg/m^3)	w/c	CMF (wt.% of cement)		SP[a] (kg/m^3)
				1MF	2MF	
Plain	1614	485	0.3	–	–	21
1MF03				0.3	–	
1MF06				0.6	–	
1MF10				1.0	–	
2MF03				–	0.3	
2MF06				–	0.6	
2MF10				–	1.0	
2MF20				–	2.0	

[a] Polycarboxylate-based superplasticizer.

suitable for this study because they would result in wall depletion at the contact planes in the case of fiber-added mixtures [35]. The rheometer was operated in a controlled room at 23 ± 2 °C and 50 ± 4% RH.

Immediately after the plastic mixture of the cement paste was loaded into the cylinder container, the two-bladed vane was positioned at mid-height of the slit with a gap size of 40 mm between the vane and cylinder base. The container was then covered to prevent the occurrence of evaporation during the test. Finally, the normal force experienced by the blades was zeroed before starting the rheometer test.

3.2. *Shearing protocol*

An optimum shearing protocol was designed for this study to minimize the shear-induced structural breakdown of cement

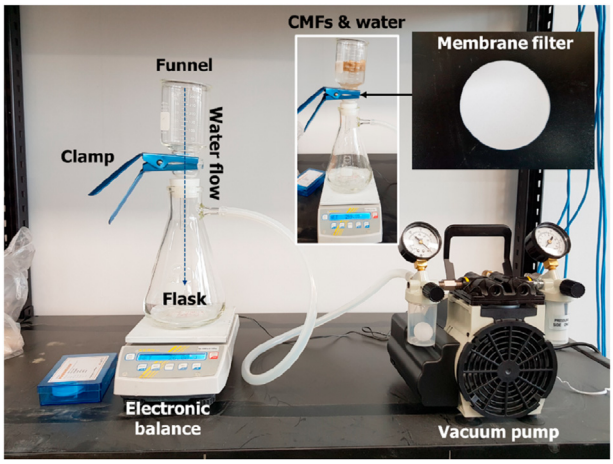

Fig. 5 – Vacuum Teflon-membrane filtration for pre-saturation of CMFs.

pastes comprising CMFs under hysteresis cycles of the shear strain rate [31]. It was observed that all the tested mixtures (Table 3) developed stable flow responses under a constant shear strain rate of 80 1/s for 300 s with no shear-induced structural breakdown. Thus, the shear strain rate of 80 1/s was selected for initial pre-shearing in the shearing protocol [36]. The designed shearing protocol (Fig. 7) comprises an initial pre-shearing step at a high shear strain rate of 80 1/s for 60 s, three acceleration and deceleration cycles from 1 to 40 1/s at steps of 5 1/s with each strain rate lasting 20 s, and a rest period at 0.1 1/s for 40 s before the initiation of each acceleration.

Following the shearing protocol, the three deceleration flow curves (i.e., shear stress–strain rate responses) were used for the analysis, with the data at 1 and 40 1/s excluded. The shear stress was measured every second, and shear stress data for each strain rate step were averaged.

3.3. *Mini-slump-flow test*

In addition to the rheometer tests, mini-slump-flow tests were conducted in compliance with ASTM C230 [37] and C1437 [38] to establish a correlation between the rheological properties (i.e., yield stress and plastic viscosity) and the spread diameter of the cement pastes comprising CMFs. The mini-slump cone had a height of 50 mm and an inner top and bottom diameter of 70 and 100 mm, respectively. A mixture of almost equal height

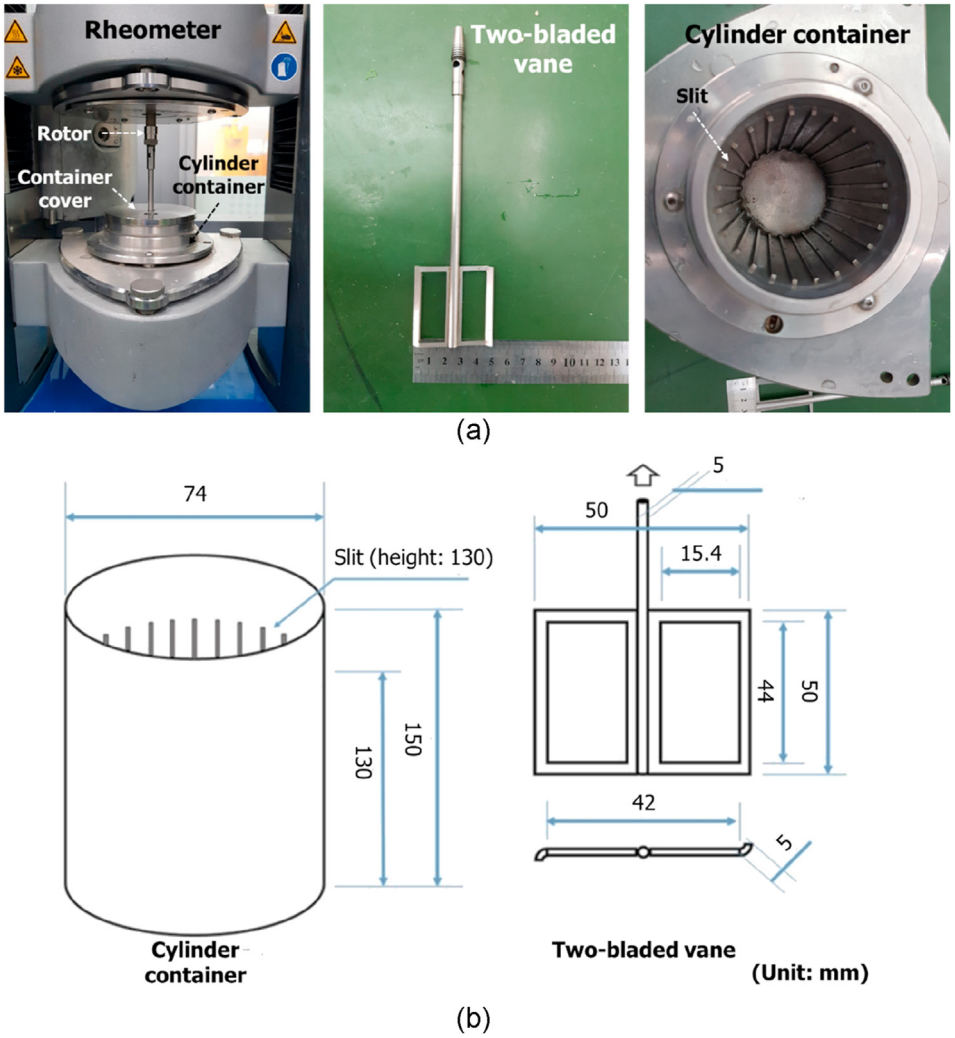

Fig. 6 – (a) Rheometer test setup and (b) geometry of cylinder container and vane.

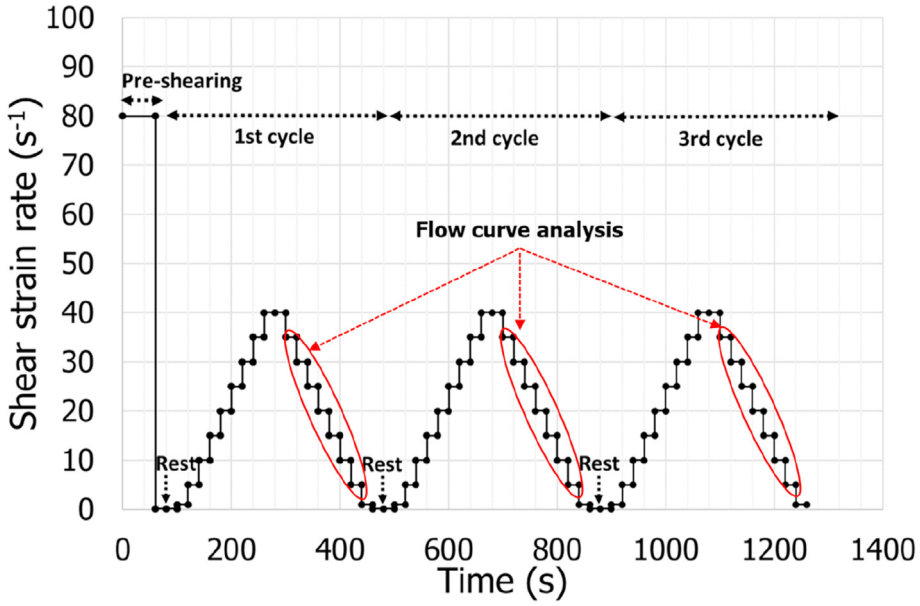

Fig. 7 – Designed optimum shearing protocol.

was poured into the cone twice with each layer being tampered 20 times using a standard rod. After the cone was raised vertically, the spread diameters of the mixture were measured in four directions to obtain the average spread diameter.

4. Results and discussion

4.1. Rheological model

The three flow curves of each mixture were fitted to the constitutive equation of the H–B model [32], which is represented by the three parameters in Eq. (1):

$$\tau = \tau_0 + a\dot{\gamma}^b \quad (1)$$

where τ, τ_0, $\dot{\gamma}$, a, and b are the shear stress, yield stress, shear strain rate, consistency index, and flow index, respectively. For $b<1$, the fluid exhibits shear thinning, whereas the fluid exhibits shear thickening for $b>1$. As this model takes into consideration three parameters, the plastic viscosity cannot be theoretically deduced. However, the equivalent plastic viscosity μ' can be calculated by applying the best approximation of the Bingham straight line to the H–B curve in a certain range of the shear strain rate [32]. Using the least squares method, the equivalent plastic viscosity μ' can be determined as follows:

$$\mu' = \frac{3a}{b+2}\dot{\gamma}_{max}^{b-1} \quad (2)$$

where $\dot{\gamma}_{max}$ is the maximum shear strain rate applied.

Under the designed shearing protocol (Fig. 7), a plain mixture and all the mixtures comprising CMFs exhibited a stable shear stress–strain rate response; Fig. 8 presents the measured shear-stress data over time for the plain mixture, as an example. This was considered as a proof of the suitability of the shearing protocol for cement pastes comprising CMFs. Based on the measured shear stress data, the relationships between the shear stress and shear strain rate were examined, as shown in Figs. 8 and 9. The shear stress plotted for each shear strain rate in Figs. 8 and 9 represents the average of the 20 data points measured at each step. For each mixture, three flow curves were fitted to the measured data based on the H–B model (Eq. (1)). It should be noted that only a shear strain rate of 35 1/s was excluded from the curve fitting of the 1MF series after observing a relatively small deviation between the measured shear stresses (Fig. 9). The rheological behaviors of the cement pastes comprising CMFs were in good agreement with the H–B model (Figs. 9 and 10).

4.2. Yield stress and plastic viscosity

According to the curve fitting, the rheological parameters and coefficients of determination of all the mixtures are listed in Table 4. In addition, Fig. 11 presents the yield stress and plastic viscosity with respect to the type and quantity of CMFs. In Fig. 11, the yield stress and plastic viscosity represent the average of the three fitted flow curves.

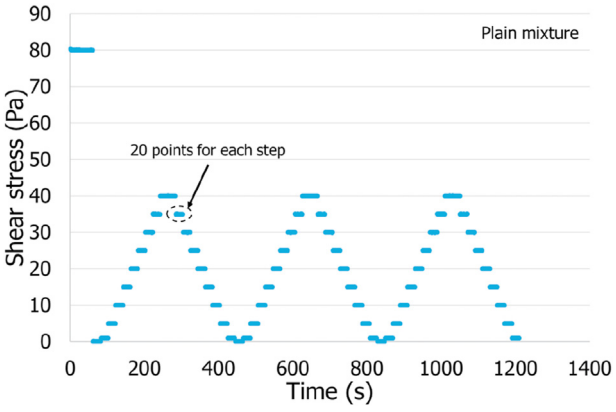

Fig. 8 – Shear stress development of the plain mixture as obtained using the shearing protocol.

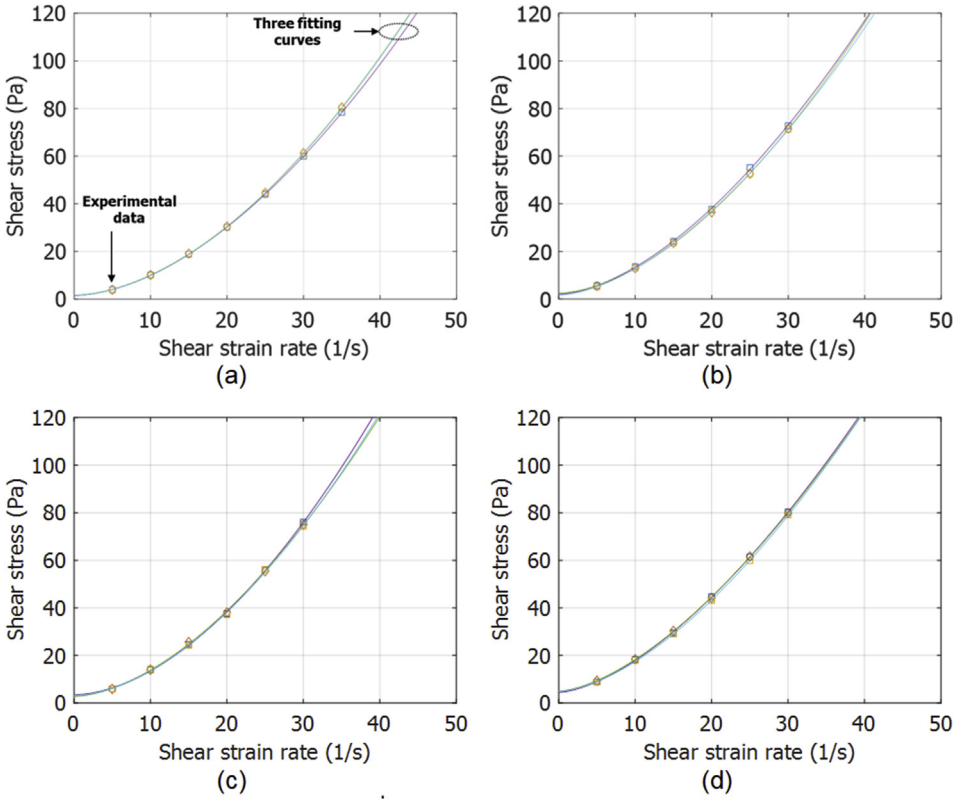

Fig. 9 – Relationships between shear stress and shear strain rate for the plain mixture and 1MF series: (a) Plain, (b) 1MF03, (c) 1MF06, and (d) 1MF10.

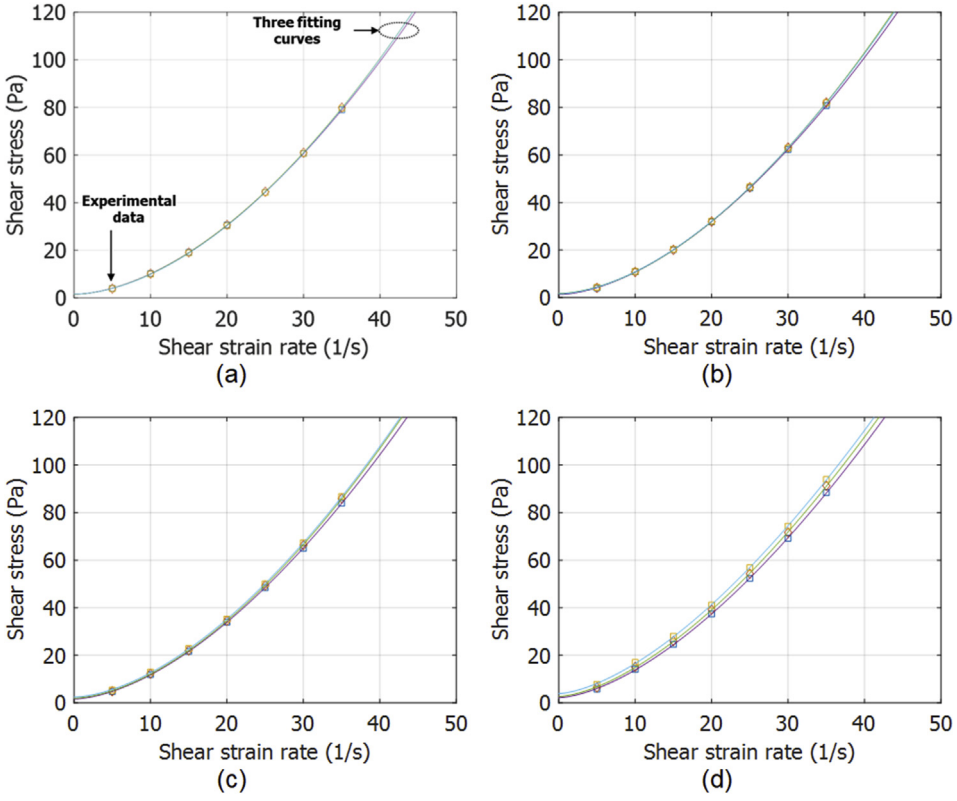

Fig. 10 – Relationships between shear stress and shear strain rate in 2MF series: (a) 2MF03, (b) 2MF06, (c) 2MF10, and (d) 2MF20.

Table 4 – Rheological parameters of tested cement pastes.

Mixture	Flow curve	τ_0 (Pa)	μ' (Pa-s)	a (Pa-s^b)	b	R^{2a}
Plain	1	1.679	1.93	0.1386	1.777	1
	2	1.919	1.97	0.1216	1.821	0.9999
	3	1.884	1.97	0.1173	1.831	0.9999
1MF03	1	2.042	1.94	0.2434	1.669	0.9997
	2	2.497	1.85	0.1920	1.730	0.9999
	3	1.643	1.89	0.2418	1.664	0.9999
1MF06	1	3.475	1.90	0.1583	1.801	0.9997
	2	2.802	1.94	0.2164	1.707	0.9996
	3	3.196	1.90	0.1766	1.765	0.9993
1MF10	1	4.514	2.12	0.3558	1.576	0.9999
	2	5.000	2.10	0.3544	1.574	0.9999
	3	4.944	2.04	0.3018	1.617	0.9999
2MF03	1	1.528	1.77	0.1516	1.754	1
	2	1.516	1.78	0.1463	1.767	1
	3	1.570	1.77	0.1379	1.783	1
2MF06	1	1.331	1.84	0.1874	1.701	1
	2	1.414	1.85	0.1732	1.728	1
	3	1.638	1.85	0.1735	1.726	1
2MF10	1	1.642	1.92	0.2166	1.670	1
	2	1.997	1.94	0.2051	1.691	1
	3	2.443	1.96	0.2115	1.684	1
2MF20	1	2.189	2.05	0.2954	1.596	0.9999
	2	2.710	2.11	0.3167	1.584	0.9999
	3	3.875	2.16	0.3461	1.564	0.9999

[a] Coefficient of determination for data fitting.

The type and quantity of CMFs had a significant influence on the yield stress of the cement pastes (Fig. 11(a)). The yield stress of the plain mixture was approximately 1.83 Pa. The inclusion of additional 1MF CMFs caused an increase in the yield stress up to approximately 4.82 Pa with 1% CMFs. The 1MF series exhibited higher yield stresses than the plain mixture. In contrast, the use of 2MF CMFs of 0.3% or 0.6% resulted in an even smaller yield stress than that in the case of the plain mixture. Furthermore, the growth rate of the yield stress with respect to the fiber dose was more drastic in the case of the 1MF series (Fig. 11(a)); the yield stress of 2MF10 was approximately 42.1% of that of 1MF10. This implies that the yield stress of the cement pastes was dependent on the length of the CMFs to a greater extent than the number of CMFs; a greater number of fibers were present in the 2MF series for a given quantity of CMFs. The increase in the interfacial friction between the granulates and fibers appeared to be marked in the case of the use of 1MF owing to its longer length as compared to that of 2MF [16]. As a reference, it has been reported in previous studies that the yield stress of the cement composites generally increases in the case of longer fibers for the same quantity [39–41].

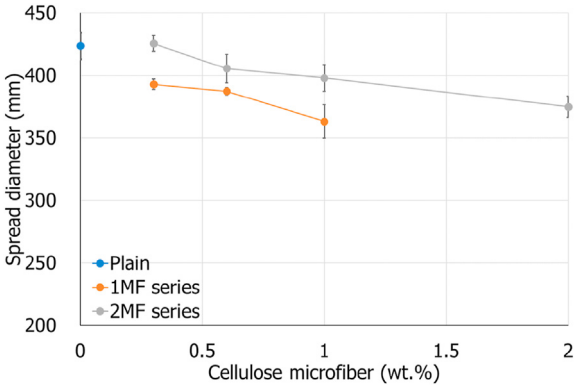

Fig. 12 – Spread diameters of tested cement pastes.

The plastic viscosity of the plain mixture was approximately 1.96 Pa-s. As a reference, the plastic viscosity of the cement paste with a w/c of 0.3 was approximately 3 Pa-s, which is in accordance with Eq. (2) [42] and is greater than that in our study owing to the exclusion of superplasticizers. In contrast to the effect of CMFs on the yield stress, all the mixtures, regardless of the presence of CMFs, exhibited a similar range of plastic viscosities with a coefficient of variation of only approximately 5.8% (Table 4 and Fig. 11(b)). This appears to indicate the adequate incorporation of CMF particles at the fiber saturation point in all the mixtures. Furthermore, 1MF03, 1MF06, 2MF03, 2MF06, and 2MF10 showed lower plastic viscosities than the plain mixture. This could be attributed to the lubrication effect of the saturated CMFs in the cement pastes, which was also observed with the use of SAPs [43,44]. Moreover, Ma et al. [45] found that the plastic viscosities of a cement paste with a w/c of 0.18 and another cement paste with the same w/c as well as SAPs saturated with extra water were nearly identical to each other. Finally, they concluded that the plastic viscosity appeared to better characterize the effect of the SAPs rather than the yield stress. The plastic viscosity increased slightly as the quantity of CMFs was increased (Fig. 11(b)). Among the two CMF series, the 2MF series exhibited a lower level of plastic viscosities.

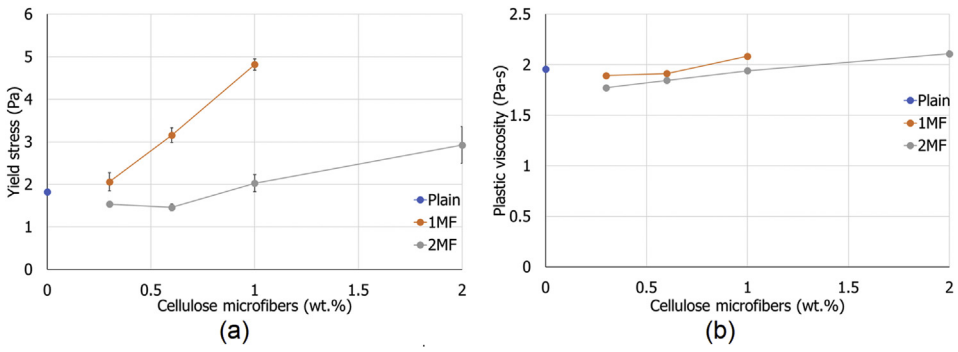

Fig. 11 – (a) Yield stresses and (b) plastic viscosities of tested cement pastes.

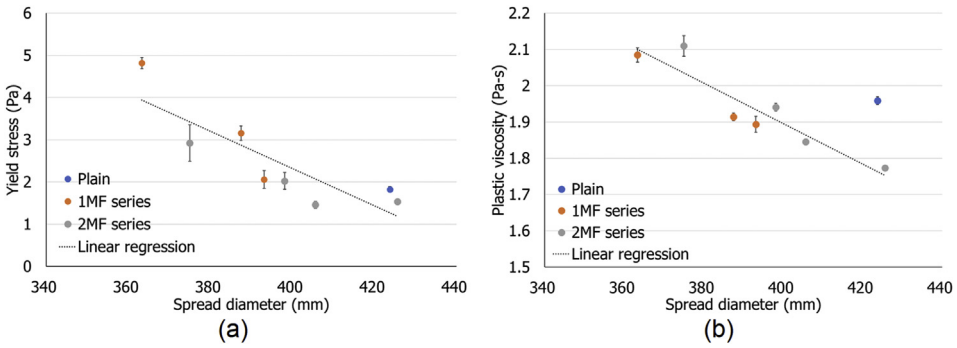

Fig. 13 – (a) Spread diameter versus yield stress, and (b) spread diameter versus plastic viscosity of tested cement pastes.

In summary, the yield stress of the CMF-added cement pastes was significantly dependent on the length of the CMFs, which would change the restraining degree of plastic mixtures. Accordingly, the minimum force required to initiate the flow of cement pastes, i.e., yield stress, is likely to vary significantly. However, the plastic viscosity appears to be considerably less affected by the length of CMFs. The CMF particles at the fiber saturation point appear to be associated with a similar plastic viscosity of the cement pastes despite the different amounts of CMFs.

4.3. *Mini-slump flow*

The spread diameter of the cement pastes comprising CMFs was affected by the length and mass fraction of the CMFs. Mixtures comprising CMFs generally exhibited a decreasing spread diameter as the quantity of CMFs used was increased. The spread diameter of the plain mixture was approximately 424 mm (Fig. 12). Except for 2MF03, the mixtures exhibited smaller spread diameters than the plain mixture. The plain mixture, 1MF03, 1MF06, 1MF10, 2MF03, 2MF06, 2MF10, and 2MF20 presented minimum spread diameters of 400, 385, 385, 360, 415, 375, 375, and 355 mm, respectively. Among the two CMF types, the 1MF series exhibited smaller flow diameters than the 2MF series. This is in accordance with the greater yield stresses and plastic viscosities of the 1MF series than those of the 2MF series.

4.4. *Relationships among yield stress, plastic viscosity, and mini-slump flow*

Both the yield stress and plastic viscosity of the tested cement pastes were analyzed with respect to the spread diameter, as shown in Fig. 13. In general, both the rheological properties of the mixtures were inversely proportional to the spread diameter, as indicated by the linear regressions in Fig. 13, although only the plain mixture did not exhibit the same trend in terms of the plastic viscosity. Among these two rheological properties, the yield stress appears to be more closely correlated with the spread diameter, regardless of the type and quantity of CMFs used. This is in agreement with the typical relationship between the spread diameter and yield stress of cement pastes [46].

5. Conclusions

In this study, the rheological properties of cement pastes comprising kenaf CMFs were investigated. The length and mass fraction of the CMFs were considered as the test variables. Prior to conducting the rheometer tests, an optimal shearing protocol was designed primarily for minimizing the shear-induced structural breakdown of cement pastes under hysteresis loops of the shear strain rate. Using the designed shearing protocol, the rheological properties of cement pastes as per the H–B fluid model were evaluated and correlated with the spread diameter from the mini-slump flow test. The summary and conclusions of this study are as follows:

1. The shearing protocol, consisting of an initial pre-shearing step at a high shear strain rate of 80 1/s, three acceleration and deceleration cycles with a maximum shear strain rate of 40 1/s, and a rest period before each acceleration, made it possible to obtain stable shear stress–strain rate responses for all the mixtures without the occurrence of a structural breakdown.
2. The yield stress of the tested cement pastes was dependent on the type (i.e., length) and mass fraction of the CMFs. The use of longer fibers (5 mm long), albeit in the same quantities, appeared to induce a larger interfacial friction between the granulates and fibers, as indicated by the drastic growth rate of the yield stress.
3. The plastic viscosities of the tested cement pastes were similar, with a coefficient of variation of approximately 5.8%. This appeared to be associated with the CMF particles at the fiber saturation point in the cement pastes, which would induce a lubrication effect between the granulates and fibers. Overall, the mixtures comprising shorter CMFs (400-μm long) exhibited a lower plastic viscosity than those comprising longer CMFs.
4. The spread diameter of the cement pastes generally decreased as the quantity of CMFs increased. Both the rheological properties of the mixtures were inversely proportional to the spread diameter, as indicated by their linear regressions. Furthermore, the spread diameter was more closely correlated with the yield stress than the plastic viscosity.

Funding

This research was supported by a grant from the Mid-Career Research Program through the National Research Foundation of Korea funded by the Ministry of Science and ICT (NRF-2018R1A2B6004546).

Declaration of Competing Interest

The authors declare that they have no known competing financial interests or personal relationships that could have appeared to influence the work reported in this paper.

Acknowledgments

The authors would like to express their sincere gratitude to Prof. Kimberly E. Kurtis at the School of Civil and Environmental Engineering at Georgia Institute of Technology for her valuable assistance in this research.

REFERENCES

[1] Market Research Future. Cellulose fiber market: information by fiber type, application and region - forecast till 2025 [homepage on the internet]. 2020 [cited 2020 Nov 10]. Available from: https://www.marketresearchfuture.com/reports/cellulose-fiber-market-2903/.

[2] Ramesh M, Deepa C, Kumar LR, Sanjay MR, Siengchin S. Life-cycle and environmental impact assessments on processing of plant fibres and its bio-composites: a critical review. J Ind Textil 2020. https://doi.org/10.1177/1528083720924730.

[3] Yashas Gowda TG, Sanjay MR, Parameswaranpillai J, Siengchin S. Natural fibers as sustainable and renewable resource for development of eco-friendly composites: a comprehensive review. Front Mater 2019;6:226.

[4] Pang C, Shanks RA, Daver F. Characterization of kenaf fiber composites prepared with tributyl citrate plasticized cellulose acetate. Compos Part A Appl Sci Manuf 2015;70:52–8.

[5] Thakur VK, Thakur MK. Processing and characterization of natural cellulose fibers/thermoset polymer composites. Carbohydr Polym 2014;109:102–17.

[6] MacVicar R, Matuana LM, Balatinecz JJ. Aging mechanisms in cellulose fiber reinforced cement composites. Cement Concr Compos 1999;21(3):189–96.

[7] Lertwattanaruk P, Suntijitto A. Properties of natural fiber cement materials containing coconut coir and oil palm fibers for residential building applications. Construct Build Mater 2015;94:664–9.

[8] Vinod A, Siengchin S, Parameswaranpillai J. Renewable and sustainable biobased materials: an assessment on biofibers, biofilms, biopolymers and biocomposites. J Clean Prod 2020;258:120978.

[9] Hemath M, Mavinkere Rangappa S, Kushvaha V, Dhakal HN, Siengchin S. A comprehensive review on mechanical, electromagnetic radiation shielding, and thermal conductivity of fibers/inorganic fillers reinforced hybrid polymer composites. Polym Compos 2020;41(10):3940–65.

[10] Yorseng K, Sanjay MR, Tengsuthiwat J, Pulikkalparambil H, Parameswaranpillai J, Siengchin S, et al. Information in United States patents on works related to 'natural fibers': 2000-2018. Curr Mater Sci 2019;12(1):4–76. Formerly: Recent Patents on Materials Science;2019.

[11] Sanjay MR, Madhu P, Jawaid M, Senthamaraikannan P, Senthil S, Pradeep S. Characterization and properties of natural fiber polymer composites: a comprehensive review. J Clean Prod 2018;172:566–81.

[12] Jongvisuttisun P, Negrello C, Kurtis KE. Effect of processing variables on efficiency of eucalyptus pulps for internal curing. Cement Concr Compos 2013;37:126–35.

[13] Bilba K, Arsène MA, Ouensanga A. Sugar cane bagasse fibre reinforced cement composites. Part I. Influence of the botanical components of bagasse on the setting of bagasse/cement composite. Cement Concr Compos 2003;25(1):91–6.

[14] Kawashima S, Shah SP. Early-age autogenous and drying shrinkage behavior of cellulose fiber-reinforced cementitious materials. Cement Concr Compos 2011;33(2):201–8.

[15] Mohr BJ, Premenko L, Nanko H, Kurtis KE. Examination of wood-derived powder and fibers for internal curing of cement-based materials. In: Proceedings of the 4th international seminar: self-desiccation and its importance in concrete Technology; June 2005. p. 229–44. Gaithersburg, MD.

[16] Galicia-Aldama E, Mayorga M, Arteaga-Arcos JC, Romero-Salazar L. Rheological behaviour of cement paste added with natural fibres. Construct Build Mater 2019;198:148–57.

[17] Ghavami K. Ultimate load behaviour of bamboo-reinforced lightweight concrete beams. Cement Concr Compos 1995;17:281–8.

[18] Sedan D, Pagnoux C, Smith A, Chotard T. Mechanical properties of hemp fibre reinforced cement: influence of the fibre/matrix interaction. J Eur Ceram 2008;28:183–92.

[19] John V, Cincotto M, Sjotrom C, Agopyan V, Oliveira C. Durability of slag mortar reinforced with coconut fibre. Cement Concr Compos 2005;27:565–74.

[20] Sanjay MR, Siengchin S, Parameswaranpillai J, Jawaid M, Pruncu CI, Khan A. A comprehensive review of techniques for natural fibers as reinforcement in composites: preparation, processing and characterization. Carbohydr Polym 2019;207:108–21.

[21] Karakoti A, Biswas S, Aseer JR, Sindhu N, Sanjay MR. Characterization of microfiber isolated from Hibiscus sabdariffa var. altissima fiber by steam explosion. J Nat Fibers 2020;17(2):189–98.

[22] Jongvisuttisun P, Leisen J, Kurtis KE. Key mechanisms controlling internal curing performance of natural fibers. Cement Concr Res 2018;107:206–20.

[23] Justs J, Wyrzykowski M, Bajare D, Lura P. Internal curing by superabsorbent polymers in ultra-high performance concrete. Cement Concr Res 2015;76:82–90.

[24] Castro J, Keiser L, Golias M, Weiss J. Absorption and desorption properties of fine lightweight aggregate for application to internally cured concrete mixtures. Cement Concr Compos 2011;33(10):1001–8.

[25] Filho R, Ghavami K, Sanjuán M, England G. Free, restrained and drying shrinkage of cement mortar composites reinforced with vegetable fibres. Cement Concr Compos 2005;27:537–46.

[26] Silva FA, Toledo Filho RD, Melo Filho JA, Fairbairn EMR. Physical and mechanical properties of durable sisal fiberecement composites. Construct Build Mater 2010;24:777–85.

[27] Boghossian E, Wegner LD. Use of flax fibres to reduce plastic shrinkage cracking in concrete. Cement Concr Compos 2008;30:929–37.

[28] Gwon S, Choi YC, Shin M. Effect of plant cellulose microfibers on hydration of cement composites. Constr Build Mater 2021;267:121734.

[29] Nilsson J, Sargenius P. Effect of microfibrillar cellulose on concrete equivalent mortar fresh and hardened properties. Swedish Cement and Concrete Research Institute; 2011.
[30] Stancato A, Burke A, Beraldo A. Mechanism of a vegetable waste composite with polymer-modified cement (VWCPMC). Cement Concr Compos 2005;27:599–603.
[31] Wallevik JE. Rheological properties of cement paste: thixotropic behavior and structural breakdown. Cement Concr Res 2009;39(1):14–29.
[32] De Larrard F, Ferraris C, Sedran T. Fresh concrete: a Herschel-Bulkley material. Mater Struct 1998;31:494–8.
[33] Han JS, Rowell JS. Chemical composition of fibers. Paper Compos Agro-based Resour 1997:83–134.
[34] Millogo Y, Aubert JE, Hamard E, Morel JC. How properties of kenaf fibers from Burkina Faso contribute to the reinforcement of earth blocks. Materials 2015;8(5):2332–45.
[35] Hubbe MA, Tayeb P, Joyce M, Tyagi P, Kehoe M, Dimic-Misic K, et al. Rheology of nanocellulose-rich aqueous suspensions: a review. BioResources 2017;12(4):9556–661.
[36] Mahaut F, Mokeddem S, Chateau X, Roussel N, Ovarlez G. Effect of coarse particle volume fraction on the yield stress and thixotropy of cementitious materials. Cement Concr Res 2008;38(11):1276–85.
[37] ASTM International. C230/C230M-20 standard specification for flow table for use in tests of hydraulic cement. West Conshohocken, PA: ASTM International; 2020. https://doi.org/10.1520/C0230_C0230M-20.
[38] ASTM International. C1437-15 standard test method for flow of hydraulic cement mortar. West Conshohocken, PA: ASTM International; 2015. https://doi.org/10.1520/C1437-15.
[39] Bentegri I, Boukendakdji O, Kadri EH, Ngo TT, Soualhi H. Rheological and tribological behaviors of polypropylene fiber reinforced concrete. Construct Build Mater 2020;261:119962.
[40] Banfill PFG, Starrs G, Derruau G, McCarter WJ, Chrisp TM. Rheology of low carbon fibre content reinforced cement mortar. Cement Concr Compos 2006;28(9):773–80.
[41] Krage G, Wallevik OH. Rheology of synthetic-fi ber reinforced SCC. In: 5th international RILEM symposium on self-compacting concrete, vol. 1; 2007. p. 347–52. Ghent/Belgium.
[42] Skripkiunas G, Karpova E, Barauskas I, Bendoraitiene J, Yakovlev G. Rheological properties of cement pastes with multiwalled carbon nanotubes. Adv Mater Sci Eng 2018;2018:8963542.
[43] Dang J, Zhao J, Du Z. Effect of superabsorbent polymer on the properties of concrete. Polymers 2017;9(12):672.
[44] Daoud M, Nasra MA. The use of super absorbent polymer as a sealing agent in plain concrete. Am J Eng Res 2014;3(3):132–7.
[45] Ma X, Yuan Q, Liu J, Shi C. Effect of water absorption of SAP on the rheological properties of cement-based materials with ultra-low w/b ratio. Construct Build Mater 2019;195:66–74.
[46] Tregger N, Ferrara L, Shah SP. Identifying viscosity of cement paste from mini-slump-flow test. ACI Mater 2008;105(6):558.